Advances in
Bridge Engineering

ORIGINAL INNOVATION

Open Access

A de-noising algorithm for bridge cable force monitoring data based on mathematical morphology

Chao Deng[1], Yi Li[2], Wei Zou[2], Yuan Ren[1*], Ying Peng[1] and Zhuo'er Han[1]

*Correspondence:
magren@126.com

[1] School of Transportation, Southeast University, Nanjing 210096, China
[2] Bay Area Super Bridge Maintenance Technology Center, Guangdong Provincial Highway Construction Co.,Ltd, Guangzhou 510699, China

Abstract

A mathematical morphological filter-based de-noising method is developed in this study for bridge cable force monitoring data. Structure elements, one of the most important parameters in the mathematical morphology, dominate de-noising effects. The de-noising effects subject to single structure element and multi-structure element filters are discussed based on the simulation signals. The results indicate that the de-noising effects by using the spherical structure element are better than using the straight line or rhombic structure element. Moreover, the multi-structure element filter outperforms the single one. Through simulation analysis, the de-noising performance of the low-pass filter, wavelet filter and morphological filter is compared. The results show that the performance of the wavelet and morphological filters is better than that of the low-pass filter. For low signal-to-noise signals, the performance of the wavelet filter is superior. With the increase of signal-to-noise ratio, the morphological filters show more advantages. Taking the cable force monitoring data of the 3rd Nanjing Yangtze River Bridge as an example, the de-noising performance of the wavelet and morphological filters is discussed. The results show that both the wavelet filters and morphological filters have satisfactory de-noising effects. The mathematical morphology method can provide an optional and effective de-nosing choice, which enriches the means of de-noising for bridge monitoring data.

Keywords: Mathematical morphology, Bridge monitoring data, Cable force, White noise, De-nosing

1 Introduction

Benefited from the rapid development of modern sensing, computing and signal processing technologies, structural health monitoring and integrity evaluation for large span bridges have become a research focus in the engineering and academic circles (Ren et al. 2019). However, monitoring signals are inevitably contaminated by noises derived from thermal, magnetic, and electrical effects of sensors and signal transmission devices (Huang et al. 2017), which cover data features of interest and disrupt the accuracy of

structural damage detection and condition assessment (Shuang Sun et al. 2021). Therefore, it is highly desired to separate noises from raw signals before data mining.

Commonly used de-noising methods include time domain averaging, low-pass filtering, wavelet-based filtering, etc. (Yadav et al. 2015). The time domain averaging involves extensive data volumes and relies on time mark information. The low-pass filtering focuses on the high-frequency feature of noises by eliminating components higher than a specific order. The wavelet-based filtering offers a higher level of details compared to low-pass filtering methods. However, the effectiveness of the wavelet-based filtering is largely dependent on the architecture of filters. Shortcomings, such as time lag and phase shift, lie in the aforementioned methods since they are developed based on time, frequency, or time-frequency domains, making it challenging to distinguish between signal and noise with overlapping frequencies (Li et al. 2016).

Mathematical morphology was derived from integra geometry and stochastic set theory, which was first used in power system and recently introduced to data mining(Gautam and Brahma 2009, 2012). The mathematical morphology filtering depends only on the local shape characteristics of signals. By means of mathematical morphological transformation, it decomposes a mixed signal into components with its main shape features (Ly et al. 2015). The mathematical morphology has been widely used in the image processing, shape analysis, pattern recognition and computer vision (Mukhopadhyay and Chanda 2000, 2002). In signal processing, mathematical morphological filters also show advantages over traditional methods for it has nonlinear characteristics, which is effective in suppressing noises such as spikes, noises, and edges. Researchers have proved mathematical morphological filters are powerful for seismic data denoising (Li et al. 2016; Huang and Wang 2018; Liu et al. 2019a). Liu (Liu and Yan 2020) found that time-frequency peak filtering performance for seismic signals could be improved by adding mathematical morphological algorithm. Moreover, for transcranial magnetic stimulation signals, Liu et al. (2022) developed a combined morphological filtering method to reduce de-noising time.

However, To the best of the author's knowledge, few research studies were reported to employ mathematical morphological filters in bridge monitoring data. Monitoring data of large span bridges such as cable force can provide key index for bridge condition assessment, which should be preprocessed with optimal filtering methods. In this paper, based on signal characteristics of bridge cable force monitoring data, the mathematical morphology theory is introduced in building a mathematical morphological filter for signal de-noising. The de-noising performance of the morphological filter is evaluated by comparing with that of the low-pass filter and wavelet-based filter.

2 Fundamentals of mathematical morphology

2.1 Basic transformations of mathematical morphology

The fundamental principle of mathematical morphology is to design a structure element (known as a "probe") to collect signal information. It is moved across the signals with the aim of matching and extracting the desired signal while preserving details and suppressing noises (Sharma and Sagar 2015). The basic operations of mathematical morphology include erosion, dilation, opening and closing. Erosion and dilation operations are associated with

identifying local minimum and maximum values, respectively. Erosion are effective in eliminating small spikes in signals, while dilation can fill the gaps. Given that bridge monitoring signals are generally one-dimensional, this study only introduces the mathematical morphological transformation in the one dimension.

The raw signal $f(n)$ is a discrete function defined on $F = (0, 1, \cdots, N-1)$, and the sequence structure element $g(m)$ is a discrete function defined on $G = (0, 1, \cdots, M-1)$ $(N \geqslant M)$. The erosion and dilation of $f(n)$ with respect to $g(m)$ are defined as follows:

$$Erosion: \ (f \Theta g)(n) = \min\ [f(n+m) - g(m)] \tag{1}$$

$m \in 0,\ 1,\ \cdots,\ M-1$

$$Dilation: \ (f \oplus g)(n) = \max\ [f(n-m) + g(m)] \tag{2}$$

$m \in 0,\ 1,\ \cdots,\ M-1$

where Θ is the erosion operator and $\oplus$ is the dilation operator. The opening and closing operations of $f(n)$with respect to $g(n)$, derived from the defined erosion and dilation operations, are defined as

$$Opening: \ (f \circ g)(n) = (f \Theta g \oplus g)(n) \tag{3}$$

$$Clo\sin g: \ (f \bullet g)(n) = (f \oplus g \Theta g)(n) \tag{4}$$

where $\circ$ and $\bullet$ denote the opening and closing operations, respectively.

2.2 Construction of mathematical morphological filters

The opening operations are beneficial for filtering peak noises and removing spikes. On the other hand, the closing can be used to smooth or reduce the valley noise, and to fill the trench-like structure (Haralick et al. 1987; Maragos and Schafer 1987). Based on the morphological opening and closing operations, three types of filters can be designed: the alternating filter, the hybrid filter and the alternating-hybrid filter.

The alternating filter is defined as

$$OC(f(n)) = (f \circ g \bullet g)(n) \tag{5}$$

$$CO(f(n)) = (f \bullet g \circ g)(n) \tag{6}$$

where OC(Opening-Closing) refers to an alternating filtering operation with opening followed by closing; and CO(Closing-Opening) is an alternating filtering that is first closing and then opening.

The hybrid filter is defined as

$$HF\big(f(n)\big) = \frac{(f \circ g + f \bullet g)(n)}{2} \tag{7}$$

where HF is a hybrid filter.

The alternating-hybrid filter is defined as

$$AH\big(f(n)\big) = \frac{\big[OC\big(f(n)\big) + CO\big(f(n)\big)\big]}{2} \tag{8}$$

where AH is an alternating-hybrid filter.

Deviation is usually seen in the alternating filter outputs since the contraction of the opening operation causes a smaller output for the OC filter. Whist, the expansion of the closing operation causes a larger output for the CO filter (Caesarendra et al. 2015). In order to address the unidirectional offset of the signal output, hybrid filters or alternating-hybrid filters are generally selected for filtering in signal processing.

2.3 Structure element

Structure elements have a great impact on the effectiveness of signal filtering. Commonly used structure elements include straight lines, rhombuses, spheres, etc. The choices of the structure elements should be determined by the signal distribution shape over time. The objective is to make its structure resembling the geometrical characteristics of the signal as closely as possible (Li et al. 2016). An example of straight line structure element is shown in Fig. 1.

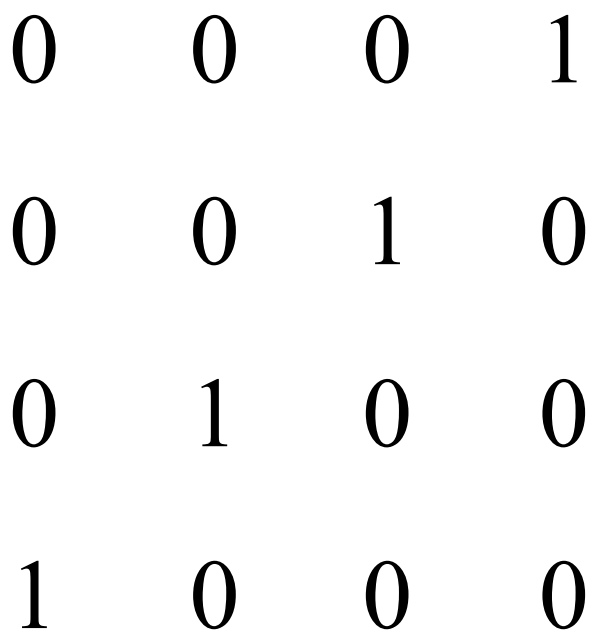

Fig. 1 Straight line structure element

3 Mathematical morphological filter design

Generally, interference signals in bridge monitoring data can be categorized into white noise interference and electromagnetic transient interference (Mo et al. 2023). Electromagnetic transient produces spiky transient waveforms in monitoring data, which can be removed by gross error elimination (Amiri and Jensen 2016). Mathematical morphological filters are designed primarily for white noise interference.

The mathematical morphological approach is based on filling detection of structure elements, the shape of which is a key factor affecting the filtering effect. The filtering effects of the straight lines, rhombuses and spheres are compared with each other in the following sections.

3.1 Single structure element filter design

The straight line structure element is determined by its length L and angle D. The rhombic structure element is determined by length L only. The spherical element is shaped by radius R and height H together.

The sampling rate of the raw signal is set as 10 Hz, where the signal is interfered by the Gaussian white noise with a signal-to-noise ratio of 15dB - Fig. 2. To determine the appropriate structure element shape and its parameter values, structure elements such as straight lines, rhombuses, and spheres are applied. Their de-noising effects are compared with each other. The effectiveness of the filtering is evaluated by the disparity between the filtered signal and the raw signal.

Mean squared errors between the filtered signal and the raw signal are used to evaluate the de-noising performance, which is expressed as

$$E = \frac{1}{n}\sum_{i=1}^{n}[sig_1(i) - sig_0(i)]^2 \tag{9}$$

where $sig_0(i)$ denotes the i^{th} value in the raw signal, $sig_1(i)$ denotes the i^{th} value in the filtered signal. The smaller the index E, the closer de-noised signal is to the raw signal, and the better the de-noising effect is. Let the variation range of L and D of the straight line

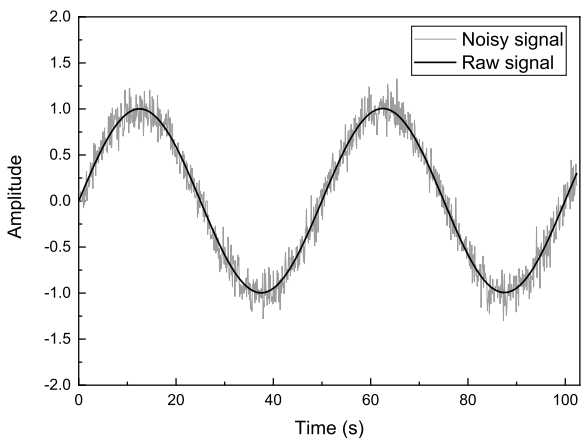

Fig. 2 Waveform of simulation signal

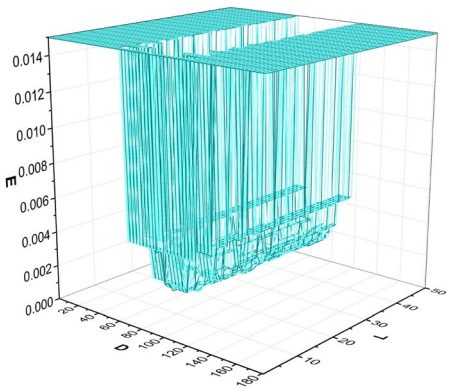

(a) Hybrid filter with straight line structure element

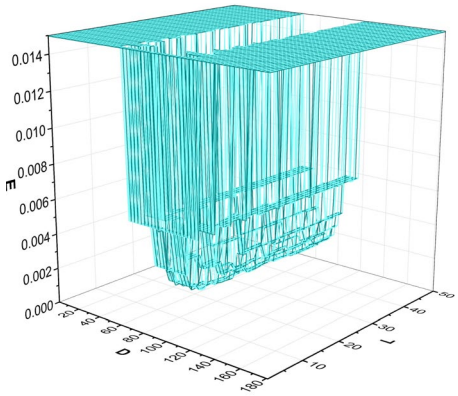

(b) Alternating hybrid filter with straight line structure element

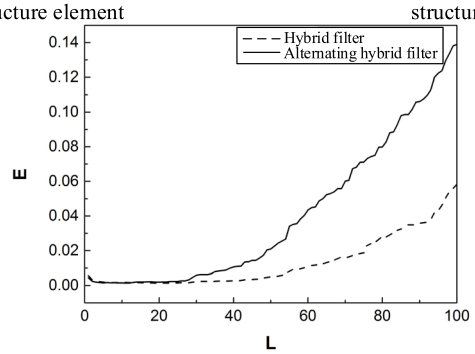

(c) Filters with rhombic structure element

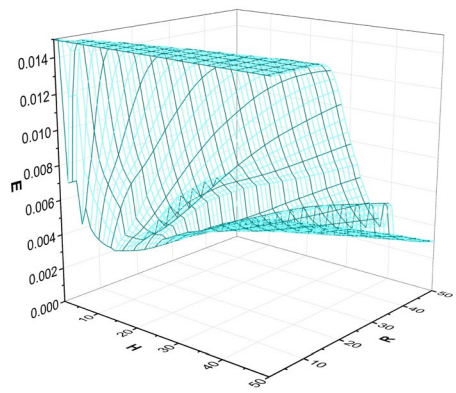

(d) Hybrid filter with spherical structure element

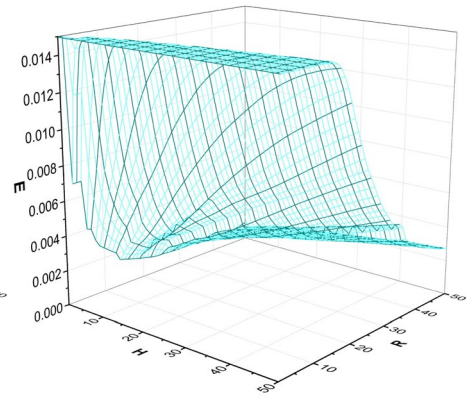

(e) Alternating hybrid filter with spherical structure element

Fig. 3 Structure element parameter analysis

Table 1 Optimal filtering effect for different types of structure elements

Structure element	Parameter	Filter type	Index *E*
Straight line	L = 40, D = 90	Hybrid filter	1.397×10^{-3}
	L = 25, D = 88	Alternating hybrid filter	1.416×10^{-3}
Rhombus	L = 20	Hybrid filter	1.397×10^{-3}
	L = 12	Alternating hybrid filter	1.416×10^{-3}
Sphere	*R* = 44, H = 1	Hybrid filter	9.78×10^{-4}
	R = 42, H = 1	Alternating hybrid filter	7.68×10^{-4}

structure element be [1,50] and [0,180], respectively, the length of the rhombic structure element L be [1,100], and R and H of sphere structure element be [1,50] and [1,50], respectively. Various parameter combinations are generated. The values of E under each parameter combination for the three structure elements are shown in Fig. 3. The de-noising effect of each type of the structure element under the optimal parameters is shown in Table 1.

The de-noising effects of the straight line and rhombic structure elements are comparable. When the optimal parameters are taken, the index E decreases to 1.397×10^{-3} at the most, no matter whether the hybrid filter or the alternating-hybrid filter. The spherical structure element performs more effectively than the other two elements. The alternating-hybrid filter has better de-noising effect, with a minimum index E of 7.6×10^{-4}. Thus, for random white noise, the filtering effect of spherical structure element is superior to that of straight line and rhombic ones.

3.2 Multi-structure element filter design

In morphological filtering process, multi-structure elements allow for nearly complete removal of noises and preserves more useful information (Li et al. 2005; Wang et al. 2005; Liu et al. 2019a, b). According to the analysis of the filtering effect of single structure elements, the spherical structure element reaches the best filtering effect with parameters of $R=42$, $H=1$. Extended from the optimal filtering results of the single structure element, multiple structure elements form a series filter in the order of size from small to large, carrying out filtering cyclically with different parameters. If the index E decreases after filtering, the filtered signal is used to replace the raw signal to continue the filtering process. Whilst, if E increases, the filtering is considered to be invalid. With the employment of the multi-structure element filter, the indicator E declined to 6.769×10^{-4}, further suppressing the signal noise level.

3.3 Simulation analysis

Noises are usually removed by using low-pass filters due to their high frequency. Moreover, wavelet technology is often applied for signal de-noising recently. Compared with the low-pass filtering, the wavelet processing method could preserve more detailed signals, leading to a better noise removal effect (Hera and Hou 2004). In this paper, Butterworth low-pass filters, wavelet filters and morphological filters are used respectively to filter simulated signals with different signal-to-noise ratios.

Gaussian white noises are added to the raw signal with signal-to-noise ratios of 5dB, 10dB, 15dB, 20dB and 25dB, respectively. The optimal cut-off frequency is determined with the optimization goal of minimizing E. In terms of wavelet filter, the wavelet basis should be first determined. Since "dB8" small basis function is the most widely used wavelet basis (Guo and He 2020; Guo et al. 2021), it is selected in this study as the wavelet basis function for de-noising. The optimal number of wavelet decomposition layers is then determined by minimizing the index E. For morphological filters, a multi-structure element filter is chosen for filtering. The optimal filtering results of different filters on signals with different signal-to-noise ratios are shown in Fig. 4.

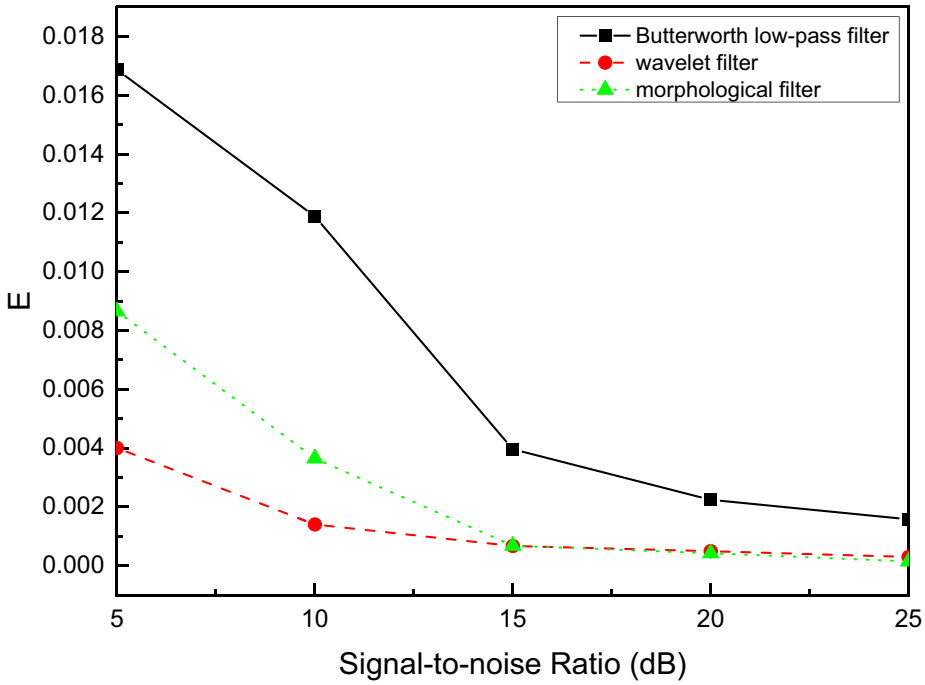

Fig. 4 Comparison of filter effect of different filters

The de-noising performance improves as the signal-to-noise ratio increases for all the three filters, i.e., Butterworth low-pass filters, wavelet filters and morphological filters. The de-noising effects of the wavelet filter and morphological filter are significantly better than that of the Butterworth low-pass filter. The de-noising performance of the wavelet filter is optimal when the signal-to-noise ratio is in the range of 5dB to15dB. While the ratio increases to within 15dB to 25dB, the morphological filter is gradually surpassing the wavelet filter.

4 Case study

The 3rd Nanjing Yangtze River Bridge is a double plane cable-stayed bridge with steel towers and steel box girders, whose main span is 648 m. The layout of the background bridge is shown in Fig. 5. The bridge was opened to traffic in October 2005. In the next year, a structural health monitoring system was devised. The system is equipped with various types of sensors, including thermal meters, anchor load cells, connected pipe systems, accelerators, etc. All the 168 stay cables are equipped with anchor load cells to measure cable forces with a sampling rate of 10 Hz. Since SA15 cable force data have high stability and reliability performance, the SA15 stay cable was selected for the filtering analysis in this study. The data were collected during the first 5 min between 8 a.m. and 9 a.m. on January 1st, 2007.

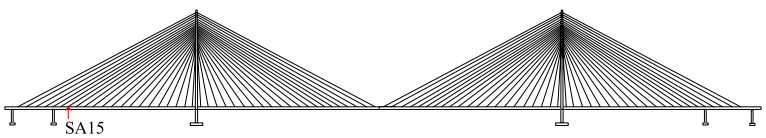

Fig. 5 Layout of the 3rd Nanjing Yangtze River Bridge

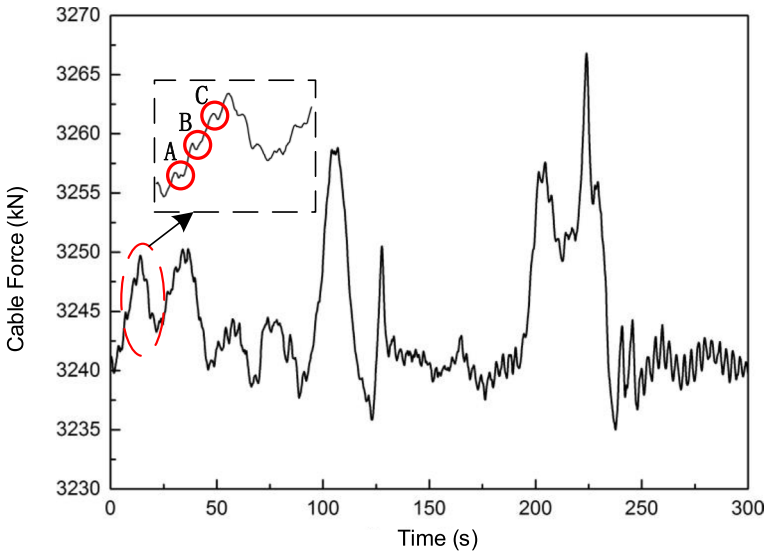

(a) Upstream cable force monitoring data of SA15

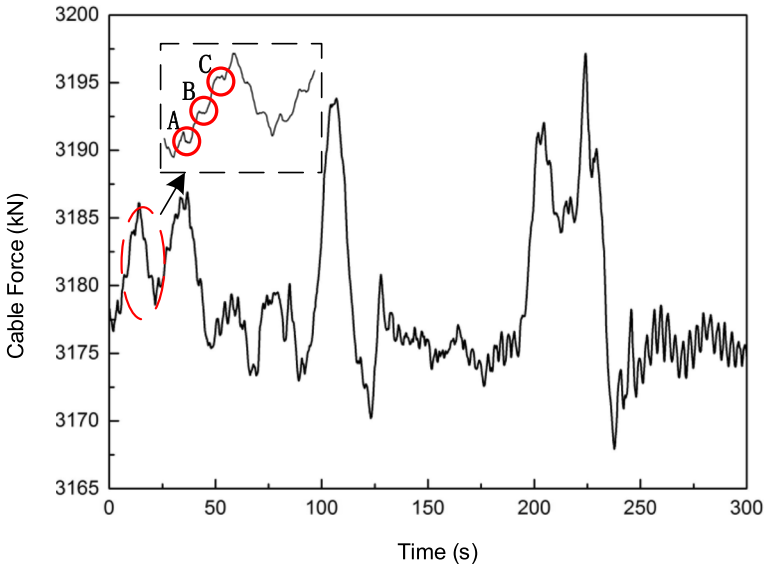

(b) Downstream cable force monitoring data of SA15

Fig. 6 Cable force monitoring data of SA15 in the transverse symmetrical positions

The upstream and downstream cable force data of SA15 are shown in Fig. 6. Signal details shown in A, B and C occur in the upstream and downstream rope monitoring data simultaneously. Due to the randomness of white noises, the detailed signals in A, B and C are impossible to be caused by noises. Moreover, they may be caused by overtaking vehicles near the studied stay cable. The motivation of this study is to remove the random white noise in the cable force monitoring signal. In this regard, it is required to retain the detailed information of the cable force caused by loads as much as possible.

Simulation analysis shows that the de-noising performance of the wavelet and morphological filters is significantly better than that of the Butterworth low-pass filters. In this regard, the wavelet and morphological filters are compared in the case study by

using field measurements. The largest difference between the field monitoring data analysis and simulation analysis is that no predictions can be made for the raw signal without noises. Therefore, the filtering effect cannot be evaluated by the index *E*. The main purpose of this study is the de-noising of white noises that are Gaussian distributions. A new index is proposed to evaluate the de-noising effect, i.e., the Gaussian fitting similarity, termed as *Adj*. The higher the Gaussian fitting similarity, the better the de-noising effect of the filter. To maximize index *Adj*, the optimal parameters for the wavelet filter and morphological filter are determined. The filtered signals of the monitoring cable forces by two filters are show in Fig. 7. The detail information in the signal is mostly preserved by using the filters.

Together with *Adj*, the root mean square error (*RMSE*), signal-to-noise ratio (*SNR*), and the correlation coefficient *R* between the de-noised signal and the monitored signal are used to evaluate the de-noising effect of the filters. *RMSE* quantifies the difference between the denoised signal and the original signal. Since the raw signal of the monitoring data is unknown, the signal and noise power are estimated through power spectral density (PSD) estimation. Smaller *RMSE*, larger *SNR* and *R* indicate a better de-noising performance. Evaluation indices of the two filters are calculated respectively, as shown in Table 2.

Both the wavelet filter and the morphological filter have good de-noising performance. For the cable force monitoring data in this study, the four evaluation indices of the morphological filter are marginally desirable than the wavelet filter, indicating that the morphological de-noising method is slightly more effective than the wavelet method.

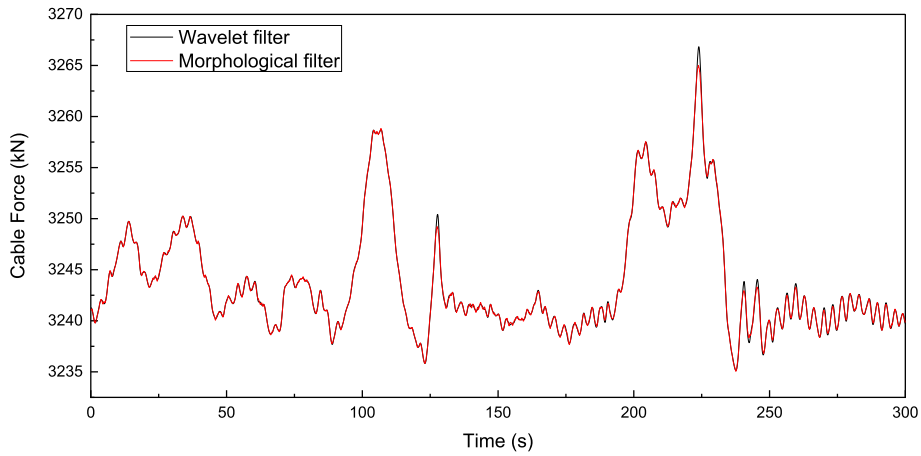

Fig. 7 Filtered signals by using the two methods

Table 2 De-noising effects of different methods

Filters	Adj	RMSE	SNR	R
Wavelet filter	0.9678	0.367295	78.92	0.9977
Morphological filter	0.9682	0.171997	85.51	0.9995

5 Conclusions

(1) An index E is proposed to evaluate de-noising effect by using simulation signals. Optimal parameters of straight line, rhombic and spherical structure elements in the mathematical morphological filter are discussed. For white noises in bridge monitoring data, the de-noising effect of the spherical structure element is better than that of straight line and rhombic structure elements. Moreover, the multi-structure element filter outperforms the single one.

(2) The de-noising effects of the wavelet filter and the mathematical morphological filter are significantly better than that of Butterworth low-pass filter through simulation analysis. The wavelet filter is dominant when signal-to-noise ratio is small. With the increase of signal-to-noise ratio, the performance of morphological filter is improving.

(3) The similarity index Adj between the noise and Gaussian distribution fitting is proposed to evaluate the de-noising effect for field measurements. Both filters have desirable de-noising effects, and the multi-structure element filtering provides an optional de-noising method for processing bridge monitoring data, enriching the means of de-noising.

Acknowledgements
The research reported in this paper was supported by the National Key Research and Development Program of China (No. 2022YFB3706704), the Academician Special Science Research Project of CCCC (No. YSZX-03-2021-01-B).

Authors' contributions
Conceptualization, Chao Deng and Yuan Ren; Methodology, Chao Deng and Yi Li; Investigation, Chao Deng, Wei Zou and Ying Peng; Writing—original draft, Chao Deng; Writing—review & editing, Yuan Ren and Zhuo'er Han; Supervision, Yuan Ren.

Funding
National Key Research and Development Program of China (No. 2022YFB3706704), the Academician Special Science Research Project of CCCC (No. YSZX-03-2021-01-B).

Availability of data and materials
The data used and/or analyzed during the current study are available from the corresponding author upon reasonable request.

Declarations

Competing interests
No conflict of interest exits in the submission of this manuscript, and manuscript is approved by all authors for publication.

Received: 29 September 2023 Accepted: 18 October 2023
Published online: 01 December 2023

References

Amiri M, Jensen R (2016) Missing data imputation using fuzzy-rough methods. Neurocomputing 205:152–164. https://doi.org/10.1016/j.neucom.2016.04.015

Caesarendra W, Wibowo D, Ariyanto M, Setiawan J (2015) An application of mathematical morphology operators as features extraction method for low speed slew bearing condition monitoring. J Robot Mech Eng Res 1:1–13. https://doi.org/10.24218/jrmer.2015.11

Gautam S, Brahma SM (2009) Overview of mathematical morphology in power systems — A tutorial approach. In: 2009 IEEE Power & Energy Society General Meeting. p 1–7

Gautam S, Brahma SM (2012) Guidelines for selection of an optimal structuring element for mathematical morphology based tools to detect power system disturbances. In: 2012 IEEE Power and Energy Society General Meeting. p 1–6

Guo J, He J (2020) Dynamic response analysis of ship-bridge collisions experiment. J Zhejiang Univ Sci A 21(7):525–534. https://doi.org/10.1631/jzus.A1900382

Guo J, Hu CJ, Zhu MJ, Ni YQ (2021) Monitoring-based evaluation of dynamic characteristics of a long span suspension bridge under typhoons. J Civ Struct Health Monit 11(2):397–410. https://doi.org/10.1007/s13349-020-00458-5
Haralick RM, Sternberg SR, Zhuang X (1987) Image analysis using mathematical morphology. IEEE Trans Pattern Anal Mach Intell 9(4):532–550. https://doi.org/10.1109/TPAMI.1987.4767941
Hera A, Hou Z (2004) Application of wavelet approach for ASCE structural health monitoring benchmark studies. J Eng Mech 130(1):96–104. https://doi.org/10.1061/(ASCE)0733-9399(2004)130:1(96)
Huang W, Wang R (2018) Random noise attenuation by planar mathematical morphological filtering. Geophysics 83(1):V11–V25. https://doi.org/10.1190/geo2017-0288.1
Huang H-B, Yi T-H, Li H-N (2017) Sensor fault diagnosis for structural health monitoring based on statistical hypothesis test and missing variable approach. J Aerosp Eng 30(2):B4015003. https://doi.org/10.1061/(ASCE)AS.1943-5525.0000572
Li H, Wang R, Cao S, Chen Y, Huang W (2016) A method for low-frequency noise suppression based on mathematical morphology in microseismic monitoring. Geophysics. https://doi.org/10.1190/geo2015-0222.1
Li Q, Wang R, Huang W, Zheng G (2005) Method for morphological filtering in seismic data processing. Pet Sci 4:24–33
Liu J, Tian K, Xiong H, Zheng Y (2022) Fast denoising of multi-channel transcranial magnetic stimulation signal based on improved generalized mathematical morphological filtering. Biomed Signal Process Control 72:103348. https://doi.org/10.1016/j.bspc.2021.103348
Liu Z, Wheaton D, Tyagi V, Wang B (2019a) Mathematical morphological filters and applications in seismic data denoising. In: 81st EAGE Conference and Exhibition 2019, London. p 1–5
Liu Z, Wheaton D, Wang B (2019b) Seismic data denoising with mathematical morphological filters. In: SEG Technical program expanded abstracts 2019, San Antonio. p 4619–4623
Liu Y, Yan Z (2020) Application of a cascading filter implemented using morphological filtering and time–frequency peak filtering for seismic signal enhancement. Geophys Prospect 68(6):1727–1741. https://doi.org/10.1111/1365-2478.12947
Ly DS, Beucher S, Bilodeau M (2015) Real-time contrast medium detection in x-ray images by mathematical morphology operators. J Electron Imaging 24(6):061202. https://doi.org/10.1117/1.JEI.24.6.061202
Maragos P, Schafer R (1987) Morphological filters–Part II: their relations to median, order-statistic, and stack filters. IEEE Trans Acoust Speech Signal Process 35(8):1170–1184. https://doi.org/10.1109/TASSP.1987.1165254
Mo C, Yang H, Xiang G, Wang G, Wang W, Liu X, Zhou Z (2023) Displacement monitoring of a bridge based on BDS measurement by CEEMDAN–adaptive threshold wavelet method. Sensors 23(9):4268. https://doi.org/10.3390/s23094268
Mukhopadhyay S, Chanda B (2000) A multiscale morphological approach to local contrast enhancement. Signal Process 80(4):685–696. https://doi.org/10.1016/S0165-1684(99)00161-9
Mukhopadhyay S, Chanda B (2002) An edge preserving noise smoothing technique using multiscale morphology. Signal Process 82(4):527–544. https://doi.org/10.1016/S0165-1684(01)00143-8
Ren Y, Xu X, Huang Q, Zhao D-Y, Yang J (2019) Long-term condition evaluation for stay cable systems using dead load–induced cable forces. Adv Struct Eng 22(7):1644–1656. https://doi.org/10.1177/1369433218824486
Sharma R, Sagar BSD (2015) Mathematical morphology based characterization of binary image. Image Anal Stereol 34(2):111. https://doi.org/10.5566/ias.1291
Sun S, Liang L, Li M (2021) Condition assessment of stay cables via cloud evidence fusion. KSCE J Civ Eng 25(3):866–878. https://doi.org/10.1007/s12205-021-0139-1
Wang RQ, Zheng GJ, Fu HZ, Li Q (2005) Noise-eliminated method by morphologic filtering in seismic data processing. Oil Geophysical Prospecting 40(3):277–282+16-372 (in Chinese)
Yadav SK, Sinha R, Bora PK (2015) Electrocardiogram signal denoising using non-local wavelet transform domain filtering. IET Signal Process 9(1):88–96. https://doi.org/10.1049/iet-spr.2014.0005

Publisher's Note